Synthesis and Characterization of a Benzoyl modified Pebax Materials for gas separation applications

Riccardo Casadei[1], Marco Giacinti Baschetti[1], Baptiste Guillaume Rerolle[2], Ho Bum Park[3], Loris Giorgini[4]

[1] Department of Civil, Chemical, Environmental and Material Engineering (DICAM) – University of Bologna, Via Terracini 28, 40131 Bologna, Italy

[2] University of Aberdeen, King's College, Aberdeen AB24 3FX, United Kingdom

[3] Department of Energy Engineering, Hanyang University, Seoul 133-791, Republic of Korea

[4] Department of Industrial Chemistry "Toso Montanari" – University of Bologna, Viale del Risorgimento 4, 40136 Bologna, Italy

Highlights

- Benzoyl group has been grafted to Pebax®2533, obtaining a new product (BP2533)
- Crystallinity of amide blocks in BP2533 disappears at high substitution degree
- Crystallinity of Polyether blocks in BP2533 increase with the substitution degree
- Gas permeability slightly increases in BP"533 with respect to pristine Pebax

Abstract

Pebax copolymers produced by Arkema are widely employed for different applications, including active molecular carriers and membranes for gas separation. In the present work, a new modification approach for Pebax®2533 is presented, as well as the characterization of the newly obtained materials.

Pebax was modified by grafting, through a nucleophilic acyl substitution, a benzoyl group on Polyamide12 block. The yield of the reaction was confirmed by FTIR and NMR analysis, while thermal DSC and TGA characterizations were then carried out on the polymeric products characterized by different degrees of substitution to understand their properties. Finally, self-standing films were obtained by casting and gas permeation tests were conducted at 35°C using CO_2, N_2, CH_4, O_2 and He, in order to understand the potentiality of the new material as membrane for gas separation.

DSC showed that in the modified Pebax, named "Benzoyl-P2533" (BP2533), the crystalline phase of the Nylon block was canceled, as expected, but at the same time the degree of crystallinity of the block of Polytetramethyleneoxide increased from 19%, measured for the unmodified Pebax, to a max of 35% for the fully substituted material. For this reason, gas permeability showed small but

consistent increment, in the order of 10-11% for most of the gas tested, with the only exception being helium, where the increment resulted to be around 48%. As a consequence, the overall selectivity of CO_2 against helium dropped with respect to pristine Pebax. For all the other gases, on the other hand the selectivity with respect to CO_2 remained substantially constant, resulting in slight but neat improvement of the ability of the new material to separate this gas.

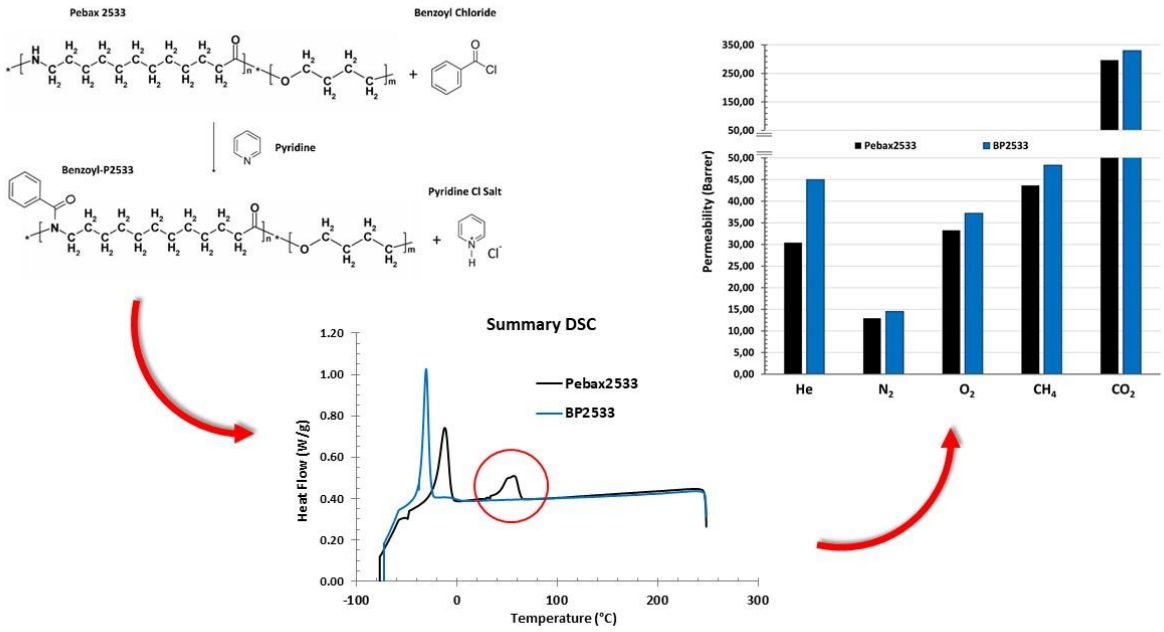

Keywords

Pebax modification; Membranes; gas permeation

1 Introduction

Pebax block copolymers, produced by Arkema, have found widespread use in different applications, from sport equipment to industrial and medical devices, thanks to the many existing grades, the tunable mechanical properties and the ease of processing. [1]-[4] In the last two decades, then, these materials become also particularly studied, in view of possible application as membranes for CO_2 capture.[5] Membranes for gas separation are known indeed to have high potential in enhancing separation performances with low installation costs and low environmental impact. [6] For this reason they have been widely studied for CO_2 separation applications, [7]-[9] both in view of the increasing attention given to global warming issues [10][11], and of the still existing economic interest in natural gas treatments [12],[14].

Unfortunately, many polymeric membranes still suffer from performance limitations which hinder their deployment in real world applications. The well-known Robeson's Upper bounds, as an example, is the graphical representation of the trade-off existing between selectivity and permeability which somewhat prevents many membrane materials, to achieve of both high separation performance and high productivity [15]. Over the years, the effort of scientific community brought to a continuous

increase of performances, but more work needs to be done to obtain further improvements and make membranes for gas separation more and more competitive with respect to other technologies. [7,14,16-20].

Different approaches are usually considered to improve the permselective performance of a membrane. It is common, for example, to employ different types of permselective fillers to enhance the gas transport properties of a standard polymeric membrane, developing the so called "Mixed Matrix Membranes" (MMM) [18, 21-23], or to produce membranes containing mobile carriers like ionic liquid or amino acids into the polymer backbone to obtain, among the others, "Ionic Liquid Membranes" (ILM) [24–27] or "Facilitated Transport Membranes" (FTM) [2,23,28-32], which both showed high potential in developing innovative membranes with high gas separation capacity. Based on these findings, the research today is mostly focused on the addition of the right fillers or carriers, in the proper amount and combination, in order to increase the overall performances of the final membrane.

Whichever is the approach considered (MMM, ILM, FTM), however, the hosting polymer chosen for the addition is of high importance in order to obtain membranes able to overcome the Robeson's upper bound. Pebax block copolymers have been often considered to that aim; they are, indeed, highly versatile materials and possess a reasonably good ability to separate CO_2 from other gases such as nitrogen or methane.[2,5,33]

Polyether block, in particular, is known to have high affinity to carbon dioxide, while the nylon moiety gives high mechanical strength and somewhat prevent the crystallization of polyether phase. High crystallinity of linear polyethers indeed strongly reduce the gas permeability, making unattractive their direct use as membrane materials. Crosslinking,[34,35] blending[36], and copolymerization [37-39] as in Pebax, are among the strategies used to create polyether based membranes for CO_2 capture.

Among the different types of Pebax available, then, the most popular for this application are surely Pebax®1657, which has been the base of many researches on membranes in the last years [33, 40-47] and Pebax®2533, endowed with a higher content of polyether blocks, which presents, lower CO_2/N_2 selectivity compared to Pebax®1657 (about 25-34 against 43-80) but higher overall permeability (for CO_2, about 130-351 Barrer against 45-80 Barrer[1]). [48-52]

Interestingly, beside their starting properties, Pebax materials present different reactive groups which can be exploited to carry on reaction that may strongly affect different characteristics of the material, such as solubility, compatibility with other chemicals/fillers, transport properties and so on. Most of the current studies, however, focus on the addition of fillers or carriers, while the possible effect related to matrix modification is subjected to limited investigation. Few works are available attempting Pebax modification in literature, like the one carried out by Yuan et al. [53] who modified Pebax®2533 by crosslinking it with Nafion to create pervaporation membranes, or Jomekian et al. [40] who investigated the possible interaction of Pebax®1657 with 3-Di-n-butyl-2-mthylimidazolium chloride (DnBMCl) ionic liquid (IL) and ZIF8.

In this context, the present work focuses on a new chemical modification of a common type of Pebax, which is reported together with the analysis of its effect on material structure and transport properties. The final goal is indeed not only related to the production of a polymer suitable to be used directly as

[1] 1 Barrer = $3.35 \cdot 10^{-16}$ mol/m/s/Pa

a membrane material, but more in general to develop a new procedure to introduce different functional groups in the polymer chains to tailor their properties and also increase their affinity with different types of filler/additives for the production of new types of gas separation membranes.

The chemical modification carried out in this work is based on the substitution of the hydrogen in the amide group of the Polyamide block with a bulky aromatic group, the benzoyl, theoretically leading to a further boost in permeability, due to the reduction of Nylon crystallinity and the subsequent increment of polymer chains mobility. In addition, Meshkat et al. [47], have recently described the use of the aromatic benzoic acid into a similar dense polymer, Pebax®1657, with interesting permselective improvements, rising CO_2 permeability and both CO_2/N_2 and CO_2/CH_4 selectivity. Thus, even if not in mobile carboxylic acid form but grafted into polymer's backbone, the addition of the aromatic benzoyl group seemed promising in term of permselective improvements.

In the present work, a thorough analysis of the reaction process and of the materials properties has been performed together with a wide characterization in term of gas permeability to have a clear view of the impact of the modification on the copolymer structure and properties. FTIR, NMR, TGA and DSC analysis have been considered and the permeability of five different gases, namely CO_2, N_2, CH_4, O_2, He, has been tested at 35°C and 1 bar of differential pressure.

2 Materials

Pebax®2533 is a block copolymer of the Pebax Thermo Plastic Elastomers family produced and distributed by Arkema S.r.l. It is made of two blocks: one of Polyamide-12 (Nylon12 or PA12) at 20 wt% and one of Polytetramethyleneoxide (PTMO) at 80 wt%. In literature, it is reported that the molecular weights of these blocks are 530 g/mol and 2000 g/mol, for Polyamide12 and PTMO, respectively [54]. The block copolymer has therefore a theoretical molar ratio of 91 mol% for PTMO and 9 mol% for Nylon12 as confirmed also by many studies reported in literature [55–59]. Pebax®2533's structure is schematized in Figure 1:

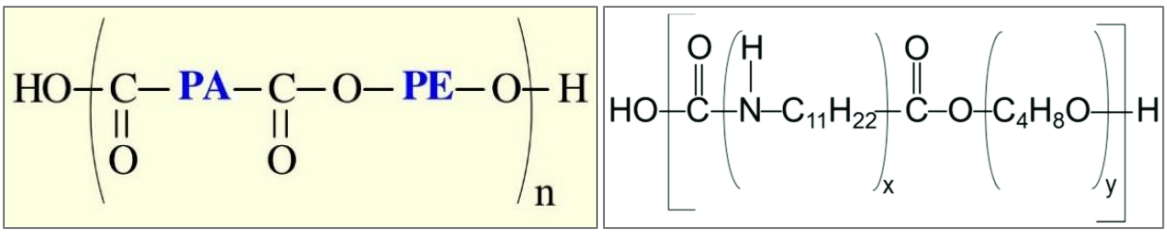

Figure 1: Pebax materials generic structure (left) [29]*, and Pebax®2533 structure (right)* [48]

All the other chemicals used in the work, Benzoyl Chloride 99%, ethanol absolute (100%), chloroform 100%, pyridine ≥99,8% and methanol 100%, were purchased by Sigma Aldrich.

The gas used for permeation tests (CO_2, CH_4, O_2, N_2, He) were chromatographic grade with 99.995 to 99,9999% purity and were purchased from SIAD spa, Italy.

3 Methods

3.1 Synthesis and Membrane Preparation

3.1.1 Synthesis of Benzoyl-P2533

The acylation reaction of Benzoyl Chloride on Pebax®2533 has been carried out in pyridine, which resulted to improve the reaction yield in three different ways: it effectively solubilized the polymer, thanks to the similar solubility parameters [60], it provided a catalytic effect for the substitution reaction,[61] and it neutralized the hydrochloric acid formed as a byproduct.[62] The overall reaction and catalyst effect schemes are displayed in Figure 2.

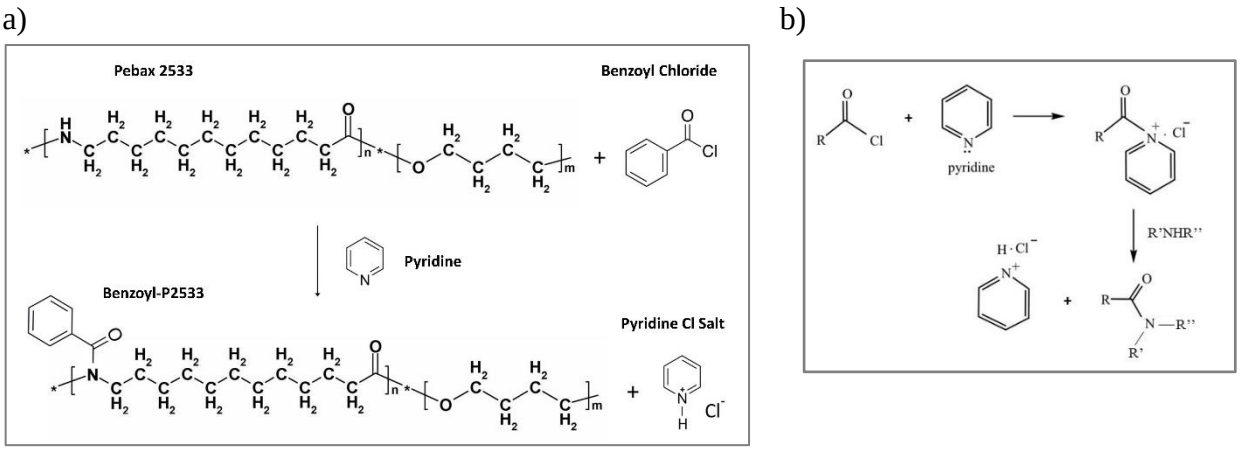

Figure 2: Schematic reaction production of BP2533 (a) and pyridine catalytic mechanism (b)

Six different protocols have been considered in order to investigate the influence of the operative conditions on the reaction yield. In particular three parameters have been varied during tests:

- Molar ratio between the amide group of Pebax®2533 and Benzoyl Chloride
- Time of reaction
- Temperature

The different parameters considered for each protocol are shown in Table 1.
Initially, Pebax®2533 was dissolved in pyridine at 2 wt% by stirring the solution overnight on a plate heated at 80°C obtaining a clear and limpid polymeric solution stable for long time also at room temperature. Then, the correct amount of Benzoyl Chloride, reported in Table1 for each different protocol, was added to the Pebax®2533 solution, and maintained under stirring condition, at 600-800 rpm, at the temperature and for the time defined in the different protocols in order to complete the reaction.
The product obtained was then separated by precipitation obtained by dropping the polymeric solution in cold deionized water (kept in ice bath, ≈ 0°C), the precipitate was then recovered and washed in excess of deionized water at 40°C for four times.
After that, the following purification steps were carried out in order to remove residual solvent and unreacted reagents:

- the product was dried in vacuum oven at 50 °C for 12 h, the temperature was then increased to 100°C and dynamic vacuum was pulled for 3 hours by maintaining the system connect to the running vacuum pump.

- the dry solid obtained was solubilized in chloroform at 30 mg/ml and slowly dropped in cold methanol (kept in ice bath, ≈ 0°C), with volume ratio of $CHCl_3$:CH_3OH = 1:3, obtaining a turbid polymeric solution
- the chloroform/methanol mixture was, in turn, dropped into cold water (kept in ice bath, ≈ 0°C), with a volume ratio of $CHCl_3$:CH_3OH:H_2O = 1:3:8, obtaining a precipitate.
- The solution was removed, and the precipitate was then dried out overnight at 50°C under high vacuum, obtaining the final solid product.

As said above, 6 different reaction protocols, reported in Table 1, were considered to understand and optimize the control of the reaction and of the degree of substitution.

Table 1: Reaction Protocols for the production of BP2533

Reaction Protocol	Material ID	Molar Ratio -NH- : BenzCl	Temperature (°C)	Time (hours)
#1	BP2533#1	1 : 2	20	2
#2	BP2533#2	1 : 5	20	2
#3	BP2533#3	1 : 10	20	2
#4	BP2533#4	1 : 5	20	24
#5	BP2533#5	1 : 5	60	2
#6	BP2533#6	1 : 10	60	4

Among the different protocols, it is possible to notice that #1, #2 and #3 were focusing on understanding the role of reactants molar ratio, which was the only parameter modified while keeping mild condition in terms of temperature and reaction time (2 hours at 20°C).

The #4 and #5 were more aggressive as a high excess of reagent was chosen (1:5) coupled with a longer reaction time (24 hours in protocol #4) or with higher reaction temperature (60°C in prot. #5).

Lastly, the most aggressive protocol, #6, has been employed with the aim of obtaining a complete substitution; for this reason, the reaction was conducted for 4 hours, with a reactants' ratio of 1:10 at a temperature of 60°C.

The product obtained by this synthetic procedure was named "Benzoyl-P2533" (BP2533).

3.1.2 Membranes Preparation

The BP2533 films were produced by solvent casting from chloroform solution obtaining self-standing and relatively thick membranes, suitable to be characterized with high accuracy.

More in details, the polymer samples were solubilized in chloroform with a concentration of 20 mg/ml; the polymeric solution was then poured in a PTFE petri dish, covered with a thin pierced aluminum foil and left under fume hood at room temperature for 3 days. When fully dried, the films were treated for 3 hours at 45°C in a vacuum oven to remove any residual solvent. The membranes were then peeled off from the Petry dish and were ready to be prepared for the different characterization experiments.

Membranes used for tests had thicknesses in the order of 80 μm, measured through a Digital Absolute Micrometer Series 227-22, Sakado, with precision of ± 1 μm. The micrometer was endowed with a disc measuring head to reduce errors while measuring soft films.

3.2 Physic-chemical Characterizations

A number of characterizations have been carried out on BP2533 films, on one side to check the success of the reaction, both qualitatively through FTIR and quantitatively through ^{1}H-NMR, and on the other side to obtain information about the structure and properties of the new materials. To that aim, crystallinity was measured using a DSC and thermal stability was evaluated by TGA; lastly, the gas transport properties were investigated through permeation experiments.

A Nicolet 380 model (Thermo Fisher Scientific, Waltham, Massachusetts, United States) was employed for FTIR analysis, by conducting attenuated total reflectance experiments with a ZnSe ATR crystal; 32 scans and a resolution of 4 cm^{-1} were used to acquire the IR spectra.

^{1}H-NMR analysis used to quantify the reaction yield for the different protocols was performed by dissolving solid samples in $CDCl_3$ at a concentration of about 5 mg/ml, which were then analyzed with a Varian Mercury Plus VX 400 (^{1}H, 399.9; ^{13}C, 100.6 MHz) spectrometer, where chemical shifts were given in ppm from tetramethyl-silane (TMS) internal reference.

TGA has been conducted, employing a Q600 model from TA Instruments, New Castle, England. All samples were prepared with weight in the range between 9 and 24 mg, and the analyses were conducted heating from 20 to 600 °C with a rate of 10°C/min, in nitrogen atmosphere to check the thermal degradation behavior of the material.

DSC analysis was performed by employing a Q2000 model from TA Instruments, New Castle, England. Samples ranging between 4 and 9 mg, were used and tested considering the following sequence of heating-cooling cycles:

- Cooling from room temperature to -80 °C (cycle 1)
- Heating from to -80 °C to 250 °C (cycle 2)
- Cooling from 250 °C to -80 °C (cycle 3)
- Heating from -80 °C to 250 °C (cycle 4)

All the cooling or heating cycles have been carried out with a rate of 10°C/min.

Gas permeation test have been conducted using a permeometer, already described in previous works [63], and schematized in Figure 3.

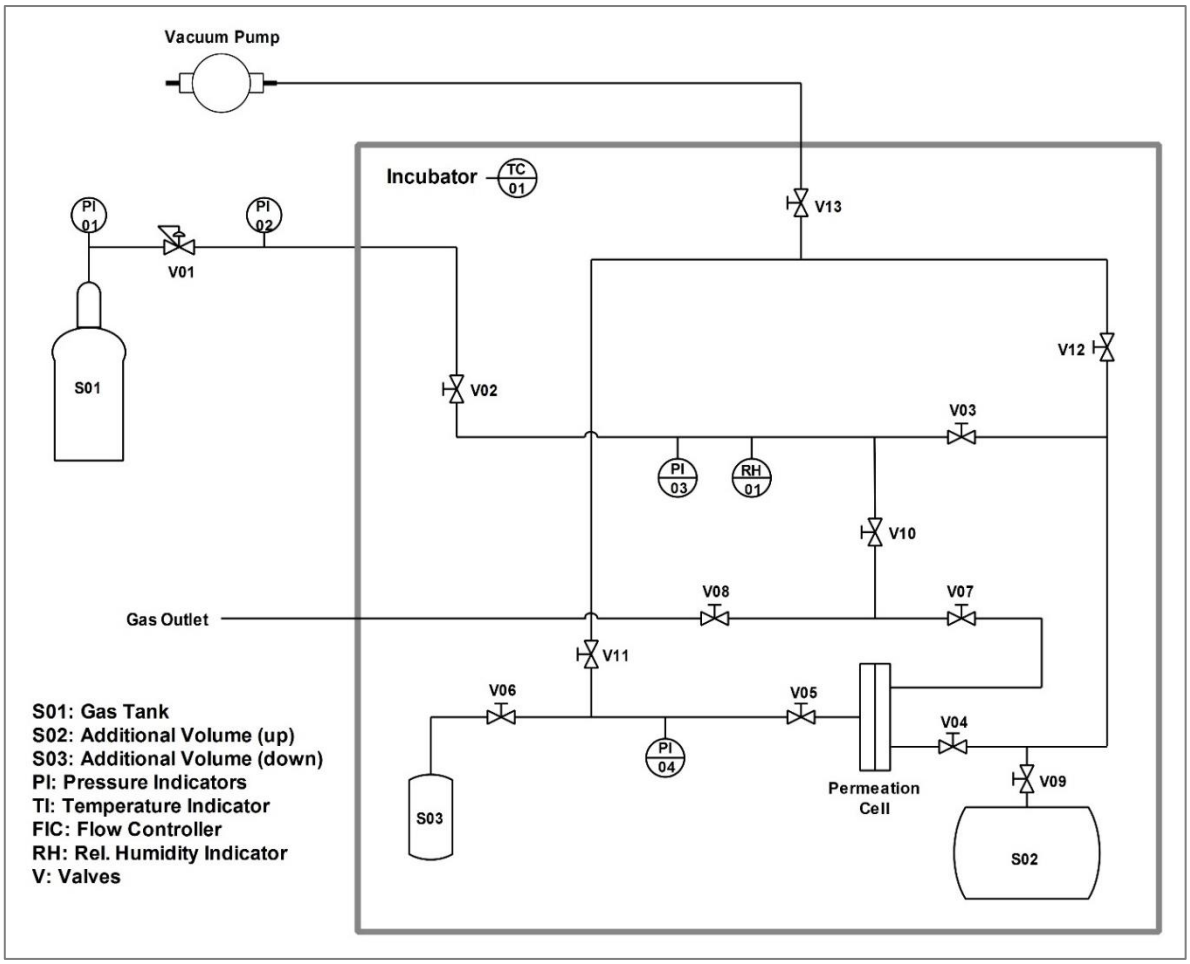

Figure 3: Single Gas Permeation System

Such system allowed to conduct single gas permeation test through a barometric technique. It was used in dry condition and at a temperature of 35°C controlled by the incubator where the whole system was contained.

Membrane selected for the tests were properly masked with an aluminum foil glued to the membrane surface with epoxy resin in order to ensure the absence of any leak in the permeation surface. The samples were then mounted in the permeation cell and high vacuum was pulled overnight from both upstream and downstream, in order to strip out any gas or vapor which could be still absorbed in the system or in the membrane itself.

Once the evacuation step was completed, 1 bar of gas was charged into upstream filling the tank S02, controlling the upstream pressure through PI03. Lastly, keeping V03, V07, V12 and V11 closed, the test was started by opening V04: at this point the gas from upstream flew to the sample cell and slowly permeated across the membrane causing a progressive increase of the pressure in the downstream calibrated volume. The pressure monitored by PI04, allowed then the calculation the permeability through Equation 1:

$$P = \left(\frac{dp_1}{dt}\right)_{t\to\infty} \frac{V}{RT} \frac{L}{A} \frac{1}{(p_2 - p_1)} \quad (1)$$

Where L represents the sample thickness, A the permeation area, V the downstream volume, T the system temperature, R the universal gas constant, and p_1 and p_2 are respectively the downstream and upstream partial pressure of the considered compound.

Overall, the maximum error on the permeability results, considering also thickness variations, volume calibration uncertainty, and other sources of error, was in the order of 5%. Unfortunately, due to the limitation of the experimental set up, which was designed for humidified gas experiments [63], the calculation of time lag for the contemporary determination of diffusivity and solubility coefficient made a reliable evaluation of these parameters not possible in the framework of the present experimental campaign. Such data were therefore not included in the present work.

4 Results and Discussion

4.1 Chemical Characterizations

Upon reaction with Benzoyl chloride, a very clear change in the physical behavior of the polymer was observed as the sample become more and more rubber like: in particular, the products of the most aggressive protocols (#3, #4, #5 and #6) resulted to be elastic, and with a strong tendency to adhere to different types of surfaces such as metal, glass, and polymers. This behavior suggests the loss of the hard, crystalline Nylon segments typical of the Pebax, that, due to the benzoyl addition, were not able anymore to crystallize nor to make hydrogen bonds.

The reaction yield and the substitution degree have been verified by FTIR and NMR analysis.

4.1.1 FTIR

The results of FTIR tests are reported in Figure 4, where the spectra of the polymers obtained through the six protocols are shown together with the one of the neat Pebax®2533. In the spectrum of the pristine polymer very clear peaks can be observed as the one at 3300 cm^{-1} related to N-H stretching, the doublet with peaks at 2925 and 2850 cm^{-1} related to C-H stretching, and the one at 1100 cm^{-1} related to C-O stretching.

In the different BP2533 spectra several new peaks appear, while others tend to vanish, with different intensity depending on the reaction protocol considered. The most clear and visible modification is surely the reduction of the N-H peak previously mentioned due to the progressive substitution of the amide's hydrogen in the pristine polymer with the benzoyl group. In addition to that, new peaks are visible at 1690 cm^{-1}, most likely related to the amide C=O bond of the new carboxylic group attached to the nitrogen, and at 700 cm^{-1} and 800 cm^{-1}, related to the aromatic C-H bending out of the benzene ring plane [64]. All the mentioned signals have been confirmed by the IR spectra of Benzoyl Chloride from NIST [65] therefore confirming the success of the substitution reaction in the different protocols.

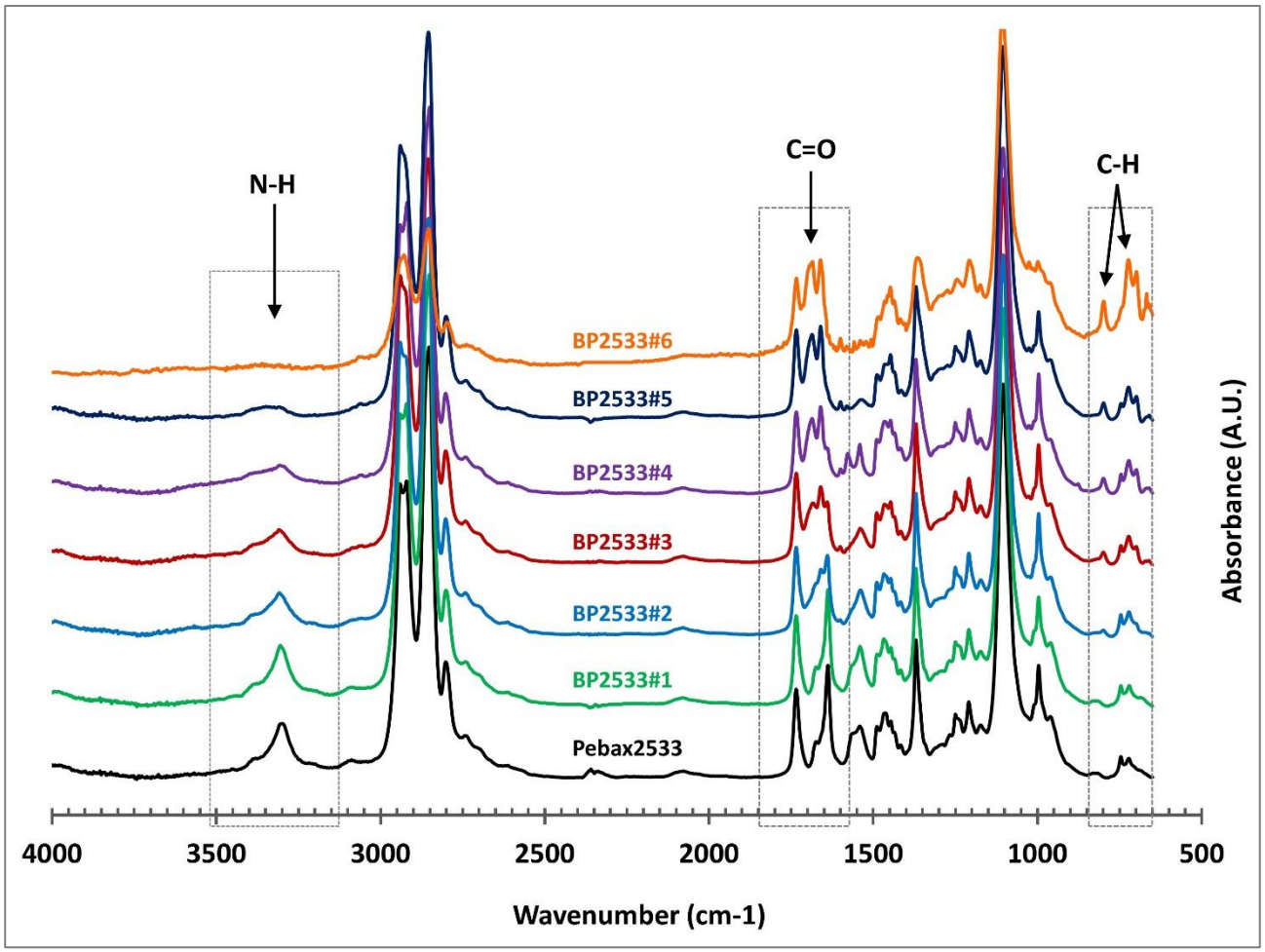

Figure 4: FTIR spectra of pristine Pebax and substituted polymeric derivatives

In particular, observing the different spectra it is already possible to obtain qualitative information about the yield of the reaction obtained with the different protocols. As an example, BP2533#1 spectrum, the mildest protocol among the six, appeared to be almost the same as the one of the neat materials thus suggesting that practically no reaction occurred.

The signal of N-H, on the other hand, clearly decreased in all the other products and overall, its intensity appears to follow the order:

P2533 ≈ BP2533#1 > BP2533#2 > BP2533#3 > BP2533#4 > BP2533#5 > BP2533#6

showing that the benzoyl substitution increases going from batch 1 to batch 6, following, as expected, the increase of concentration of the Benzoyl Chloride in the reaction environment as well as the increase of the reaction temperature and time. In particular, the N-H related signal (at 3300 cm^{-1}), which is already rather small in BP2533#4 and #5, seems to vanish in BP2533#6, which should be therefore very close to complete substitution.

4.1.2 ^{1}H-NMR

To verify the quantitative yield of substitution, ^{1}H-NMR analysis has been conducted on all the different materials considered. ^{1}H-NMR spectra of Pristine Pebax®2533 and highly substituted BP2533#5 are shown in Figure 5 and 6 respectively as an example of the obtained results. The full spectra is reported together with an inset in the aromatic range (from about 7 to 8 ppm) where the main evidence of the reaction are visible.

In the aromatic range of the BP2533#5 spectrum it is indeed possible to see three signals, absent in the pristine polymer, which are in line with the structure of the benzoyl group inserted: the orto and metha hydrogens of the benzene ring, indeed, are symmetric, producing overall one signal each, while the third signal is related to the para hydrogen. The five aromatic hydrogens have been taken into account to integrate the NMR signal (Figure 7 $H^{(16)}$, $H^{(17)}$, $H^{(18)}$, $H^{(19)}$, $H^{(20)}$) to quantify the reaction yield. The overall area was considered as the peaks are partially superimposed and have low intensity, which is in agreement with the fact that the reported mass ratio is 80/20 PTMO/Nylon, with the theoretical mole ratio even lower: about 91/9 PTMO/Nylon, considering the structure for Pebax material reported in Figure 1, provided by Arkema [2], as molecular weight reference calculation.

Such sum of signals has been compared with the signal of the four -CH_2 hydrogens at 3.4 ppm (Figure 7, $H^{(12)}$ and $H^{(15)}$), of the PTMO block that form an overall very intense single signal. These have been preferred because the signal is cleaner and without interferences or shoulders, compared to the other four inner hydrogens ($H^{(13)}$ and $H^{(14)}$ in figure 7), at 1.60 ppm. The results of such comparison are reported in Table 2.

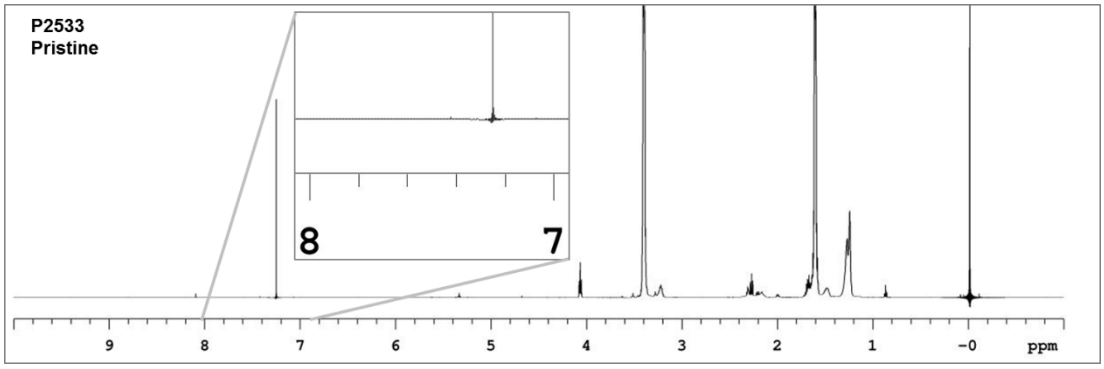

Figure 5: ^{1}H-NMR signal of Pebax®2533. The inset in the spectrum range between 7-8 ppm refers to aromatic region where no peaks are present.

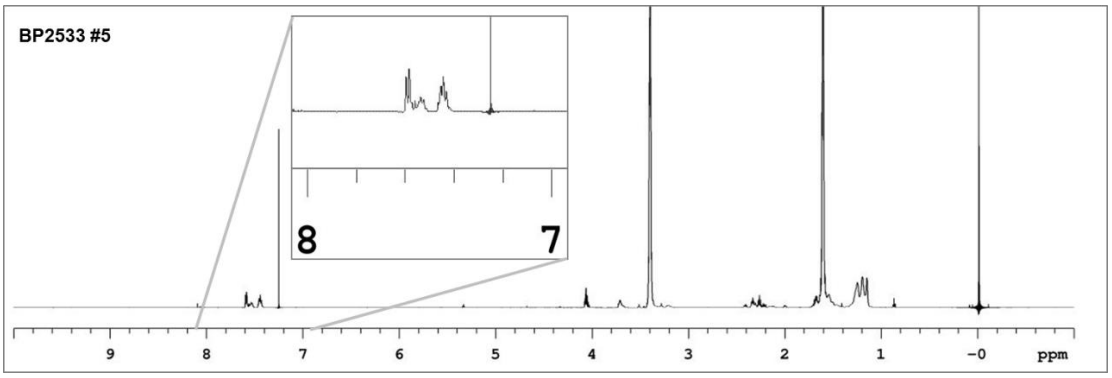

Figure 6: ^{1}H-NMR signal of Benzoyl-P2533#5 The inset in the spectrum range between 7-8 ppm refers to aromatic region where peaks of benzoil aromatic hydrogen are visible ($H^{(16)}$, $H^{(17)}$, $H^{(18)}$, $H^{(19)}$, $H^{(20)}$ in Figure 7)

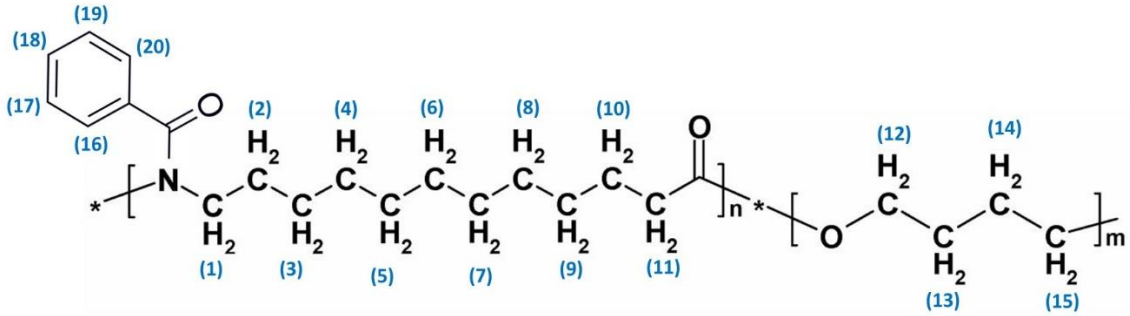

Figure 7: Benzoyl-P2533 (BP2533) chemical structure

Table 2: Summary of molar substitution degree % results

Material	Molar Substitution degree %
Pebax®2533	/
BP2533#1	~ 0
BP2533#2	25
BP2533#3	42
BP2533#4	66
BP2533#5	68
BP2533#6	99

From the table, it is possible to notice that the substitutions obtained resulted to be in line with the FTIR spectra evaluations: for the mildest protocol #1, no aromatic signal have been detected; while the results of the other materials follow the N-H signal's intensity of the FTIR spectra previously presented in Figure 4, with the molar substitution presenting the same order:

BP2533#1 < BP2533#2 < BP2533#3 < BP2533#4 < BP2533#5 < BP2533#6

The last three protocols showed the highest substitution yield: 66% and 68% for #4 and #5 respectively, and 99% for #6, that as already hypothesized, resulted basically fully substituted.

Using once again Figure 1 as a reference, the experimental mass ratio resulted very similar to the reported one: 79 wt% Polyamide12 and 21 wt% PTMO (instead of 80/20), for the analyzed Pebax®2533.

4.2 Thermal Characterizations

4.2.1 TGA

To investigate thermal properties of the materials obtained, TGA was conducted, on the different samples. The obtained thermograms are shown in Figure 8 where an inset in the range 250-450°C has been also added to better clarify the behavior of the different materials at the beginning of the degradation.

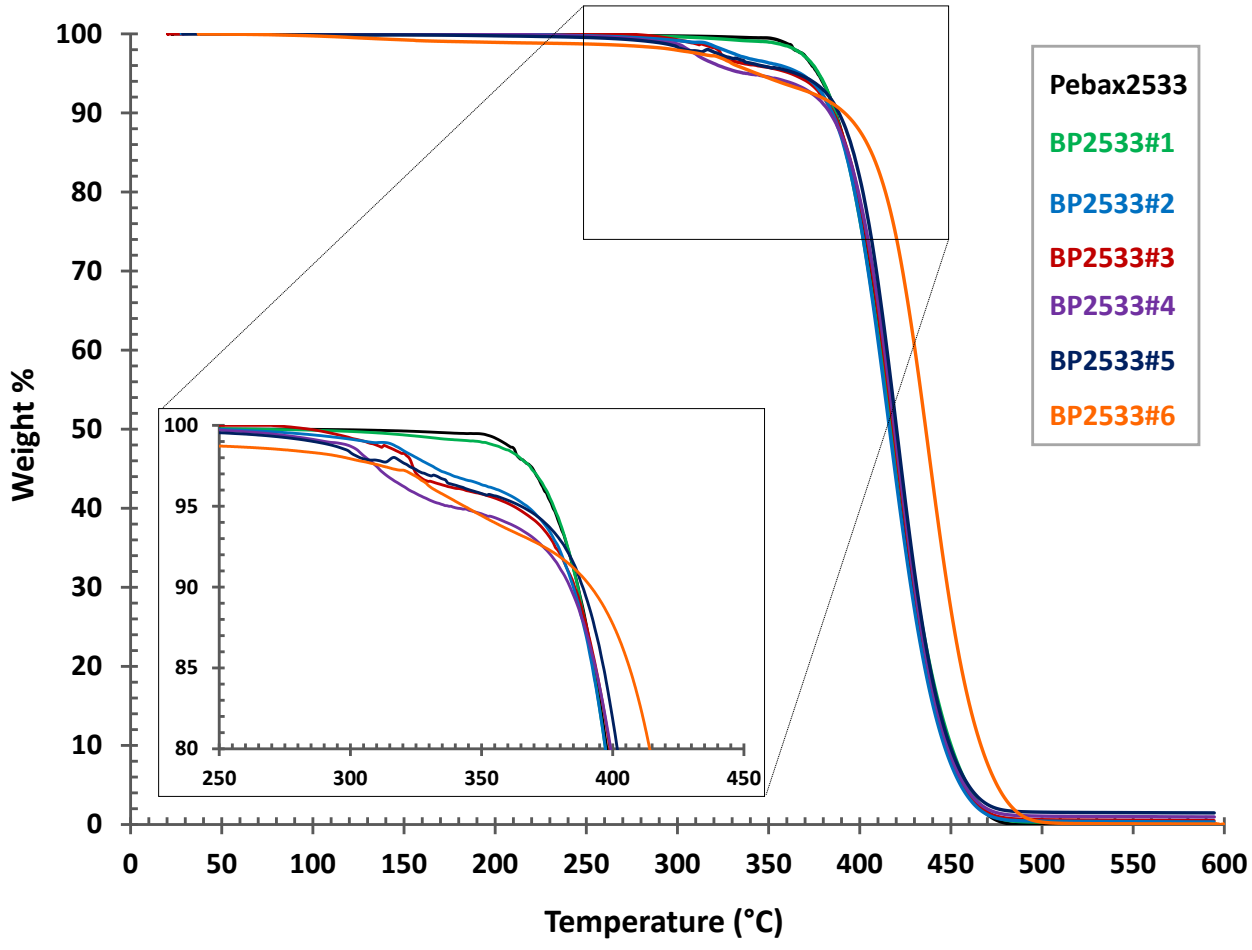

Figure 8: TGA results for the different investigated materials. The inset shows the weight loss in the range between 250 and 450°C

Pebax®2533, along with the protocol #1 (≈ 0 mol% substitution material), start to degrade at 360°C (Figure 8) and present a single degradation step. All the other samples degrade at lower temperatures, around 275°C, showing an additional degradation step before 360°C when the polymer chain degradation begins. Interestingly, this initial weight loss is consistent with the substitution degree, as

the materials with higher substitution showed higher weight loss between 275 and 360°C, from 0 wt% loss for sample #1, to 7 wt% for sample #6.
It is also interesting to notice that the fully substituted sample #6 exhibits a notable change in the polymer chain degradation that results shifted of about 20 °C towards higher temperature, as easily notable especially during the degradation after 400°C.
In conclusion, such materials do not seem to have particular thermal limitations for the most common applications as, for example, polymeric membrane separation processes are usually far below 200 °C.

4.2.2 DSC

To further check the thermal properties and evaluate the degree of crystallinity of the two polymeric blocks, DSC analysis has been conducted following the procedure previously described. In Figure 9 the curve related to the 3rd cooling and 4th heating cycles are displayed for all the products investigated.

For the pristine Pebax®2533, as expected, the crystallization and melting signals for both Nylon12 block (about 55°C and 140°C, respectively) and polytetramethyleneoxide (about -10°C and 10°C, respectively) are clearly visible in Figure 9; no visible glass transition temperatures, Tg, are instead present in the thermograms, as for PEBAX2533 a Tg in the order of -65°C is reported [66], that is around the minimum temperature (-80°C) investigated in the present work.

Interestingly, the melting point of Nylon12 resulted lower than values usually reported in literature, which are around 180°C [67-71]. Such difference is most likely due to low the molar weight of Nylon block in the copolymer as well as its quantity in the material which is also rather low, as pointed out above, thus influencing the structure of the crystalline phase and its melting temperature.

Nylon12 crystallization and fusion signals are, then, visible only in the pristine material and protocol #1 samples, while from protocol #2 and above basically no Nylon fusion peak occurred. This behavior is due to the insertion of the benzoyl group that, by decreasing the structural order, prevents the crystallization of the Polyamide macromolecular chains.

Another peculiar trend is that the crystallization signals of PTMO block fall at lower temperatures when the substitution of benzoyl occur (from sample #2 and above), so that such materials cannot complete their very crystallization during the cooling and make it in the successive cycle 4 of heating where more and more evident crystallization peaks can be observed before melting.
Such delay in the crystallization process with the increment of the substitution is another effect of the bulky group inserted, which increases the disorder and the free volume available for the macromolecular chains of PTMO, which therefore require more time to reorganize in the crystalline phase. From another point of view, it can be said that Nylon12 crystals and the hydrogen bonds network present in pristine Pebax®2533 facilitated the chain alignment thus promoting the ordering of the PTMO blocks in a crystalline structure, an effect which is lost in the modified material.

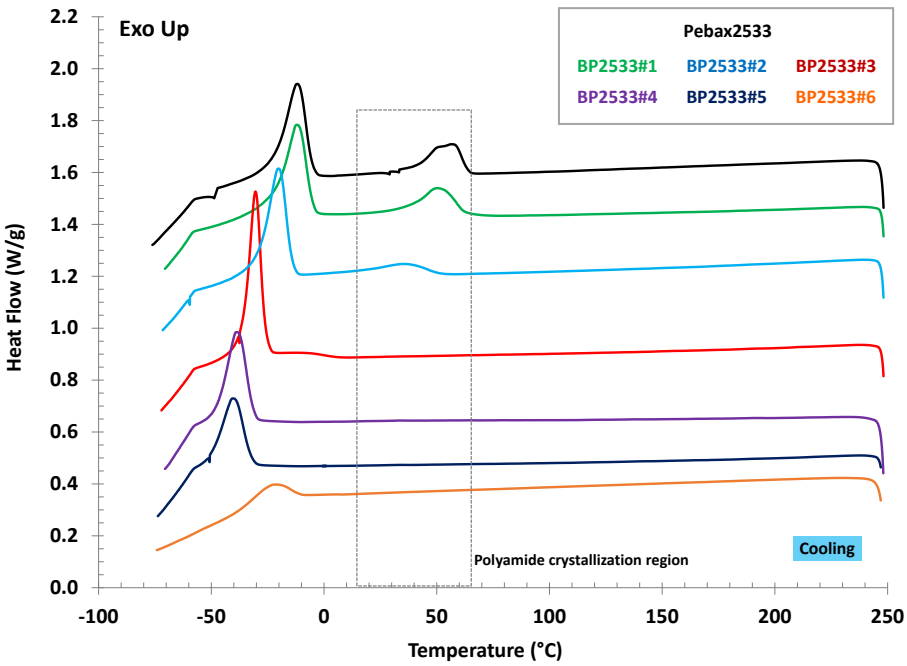

a)

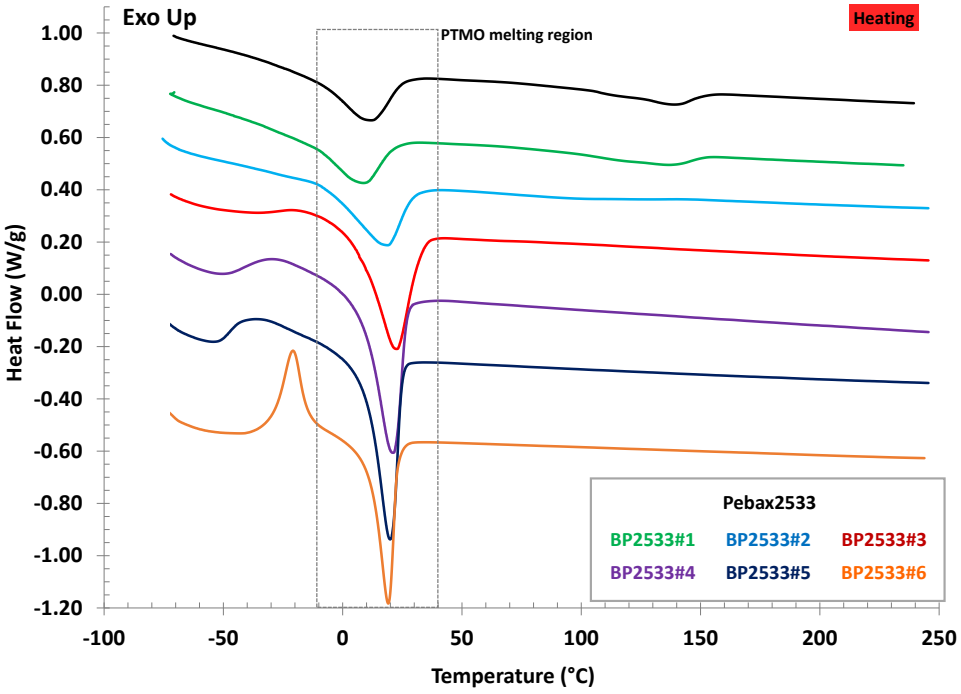

b)

Figure 9: DSC Thermograms of the investigated polymers a) cooling cycle, b) heating cycle

The amounts of crystalline phases were calculated from Figure 9 by using the following Equation 2:

$$Crystallinity_i\% = \frac{\Delta H_i^{m_{exp}}}{\Delta H_i^{m_0} \cdot y_i} \cdot 100 \quad (2)$$

Where *i* is one of the two moieties (Nylon12 or PTMO), $\Delta H_i^{m_{exp}}$ was the melting enthalpy obtained experimentally, $\Delta H_i^{m_0}$ the melting enthalpy of a 100% crystalline compound *i*, y_i was the mass fraction in the polymer obtained from NMR (0,214 for Nylon12 and 0,786 for PTMO).

To calculate the integrals of the peaks, signals of 4th cycle of heating have been chosen, while the melting heat references considered were 209,3 J/g for 100% crystalline Nylon12 [72] and 167,0 J/g [73] for 100% crystalline PTMO.
Detailed results are listed in Table 3, which confirm the disappearance of the Nylon crystalline phase and reveal the increment of PTMO crystallization with the substitution. This change, which bring the crystallinity of the polyether phase from 19% for the pristine PEBAX to a maximum of almost 35%, is an interesting result, as it seems that while slowing down the crystallization process the addition of benzoyl groups actually increases the overall crystallinity of the substituted materials. On one side, therefore, the bulky aromatic ring seems to delay the nucleation process of PTMO crystals, but, on the other hand they also provide more space for the crystals to grow thus reaching higher crystallization degree. Such effect is active until a substitution degree around 40% (protocol #3) is reached; indeed, from this point on, and up to the fully substituted material (#6), the crystalline fraction in PTMO increases of less than 3%, from 32 to almost 35%.

Table 3: DSC results for the different materials inspected

Sample	T peak PTMO (°C)	ΔH peak PTMO (J/g)	T peak Nylon (°C)	ΔH peak Nylon (J/g)	Ratio Peak P/Ny	Cryst degree PTMO (%)	Cryst degree Nylon (%)
Pebax®2533	11,3	25,3	138,2	8,3	0,33	19,3	18,6
Benzoyl P2533 #1	10,1	24.0	137,4	8,3	0,34	18,3	18,5
Benzoyl P2533 #2	18,6	27,7	-	-	-	21,1	-
Benzoyl P2533 #3	22,6	42,4	-	-	-	32,3	-
Benzoyl P2533 #4	21,1	43,4	-	-	-	33,0	-
Benzoyl P2533 #5	19,9	42,7	-	-	-	32,6	-
Benzoyl P2533 #6	19,1	45,8	-	-	-	34,9	-

4.3 Gas Permeation Characterizations

Gas transport characterization have been conducted using CO_2, N_2, CH_4, He and O_2, in single gas permeation experiments as described in section 3.5.

Due to its stickiness and rubberlike response, the fully substituted BP2533#6 self-standing membranes were very difficult to be handled and could not be used in the permeation tests. As a consequence, it was chosen to focus on BP2533 obtained using a protocol #5; with a molar substitution of 70%, this material was still manageable, likely due to the resistance of a limited hydrogen bonding network formed by the residual Nylon amine groups, and represented a good compromise between the substitution degree, related to the expected permeability increase, and the material testability. For comparison, also permeability of pristine Pebax®2533 was measured.

In Figure 10 the overall permeability results of tested gases are shown, while in Figure 11 the ideal selectivity to CO_2 is reported. For clarity, then gas permeation results of Figure 10 and 11 are more precisely listed in Table 4, along with the uncertainty interval related to experimental errors. .

From the permeation results obtained, it is clear that, even considering the uncertainty of the measurements, the modification of the polymer slightly increased the overall permeability of the system: the increment in terms of average value was about 11-12 % for all gases except helium, where the permeability improved by 48 % with respect to the one measured for the pristine Pebax®2533.

All gases except helium shared also the same behavior for the CO_2 selectivity, which indeed remained basically constant with respect to pristine material (variation in the range of -0,5 % and + 0,4 %); for helium, instead, it decreased of about 25%, as a consequence of the different permeation trend of the latter gas with respect to the others.

The general permeability increase observed in BP2533 is probably due to the higher mobility of the substitute copolymer chains that can favor the gas permeation within the matrix; the substitution indeed decreased both crystallinity and polyamide rigid hydrogen bonding network while it increased the polymer free volume due to the bulkiness of the added benzoyl group.

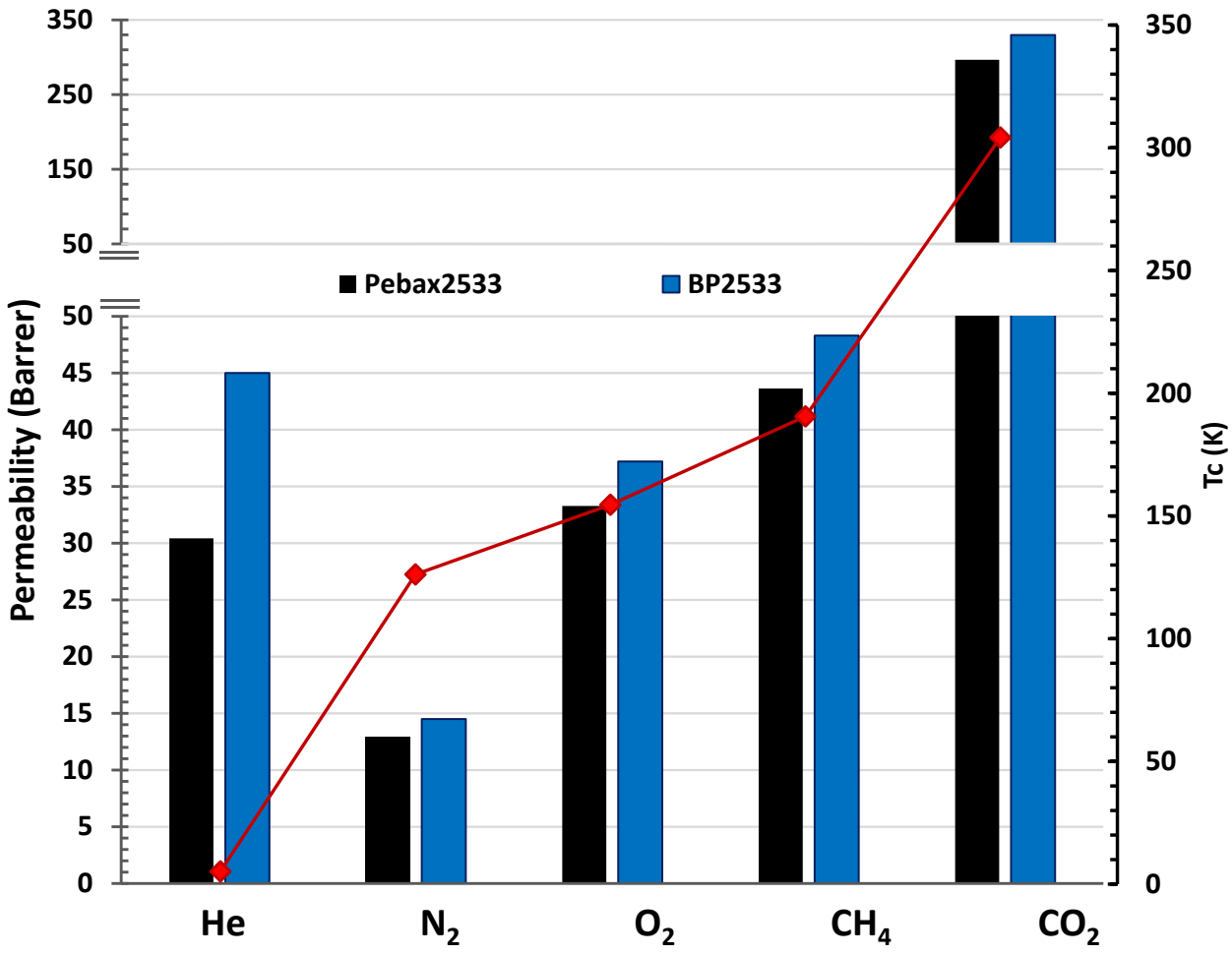

Figure 10: Pebax®2533 and Benzoyl-P2533#5 (70 mol%) Permeability results and relationship with gas critical temperature (indicated by the solid red squares)

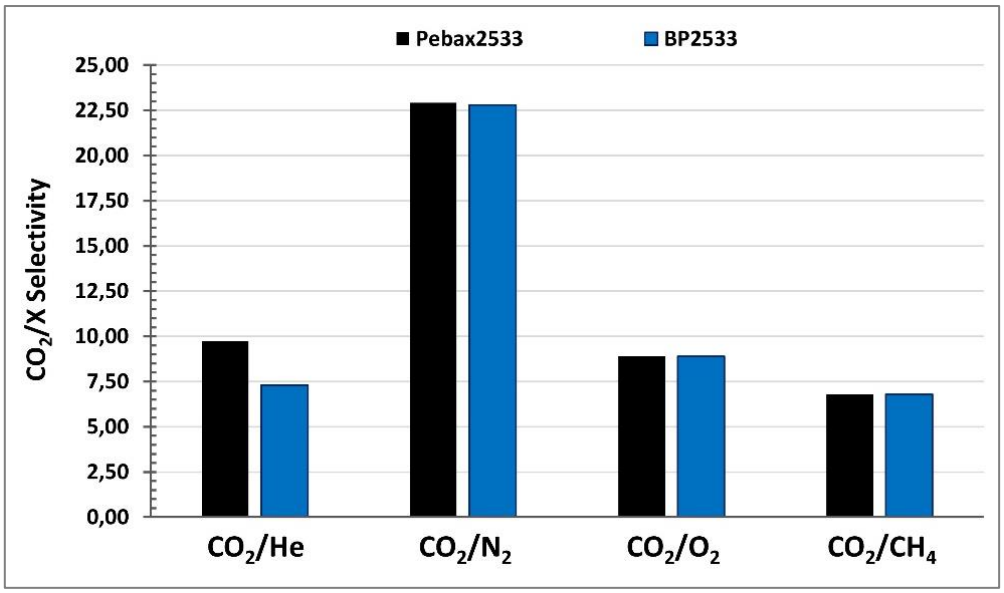

Figure 11: Pebax®2533 and Benzoyl-P2533#5 (70 mol%) Selectivity results

Table 4: Pebax®2533 and Benzoyl-P2533#5 (70 mol%) gas permeation summary

	Pebax®2533					BP2533#5 (70% conv.)				
Gas	CO_2	CH_4	O_2	N_2	He	CO_2	CH_4	O_2	N_2	He
Permeability (Barrer)	296± 15	43±2	33± 2	12 ±1	30 ±2	330± 16	48 ±3	37 ±2	14 ±1	45 ±3
Selectivity CO_2/X	\	6,8	8,9	22,9	9,7	\	6,8	8,9	22,8	7,3
Critical Temp. (K)	304.2	190.6	154.6	126.2	5.2	304.2	190.6	154.6	126.2	5.2
Kinetic Diam. (pm)	330	380	346	364	260	330	380	346	364	260

In this concern, to better investigate the behavior of the different gas within the polymer from a permeability point of view, in Table 4, the critical temperature (T_c) and kinetic diameter of all tested gases are reported as well. Considering the solution diffusion mechanism, indeed, permeability will depend on both thermodynamic (solubility parameter) and kinetics (diffusivity) factors, which are often known to scale respectively with gas condensability (related to T_c) and molecular dimensions (expressed through the kinetic diameter). Analyzing the behavior with critical temperature, also reported in Figure 10 for clarity sake, it is possible to notice that the permeability of all gases (except helium) increase with the increment of Tc, for both neat Pebax®2533 and BP2533#5. This does not seem the case for the comparison with kinetic diameters, where no trends are appreciable. This result seems to indicate that the solubility parameter is dominant for these materials, in respect to the diffusivity one.

Interestingly, as noticed above, helium results to be outside the trends followed by all the other gases, generally showing higher permeability than what expected from its low condensability. This fact may be related to its dimensions, definitely smaller than any other gas, which make the diffusivity factor count as well in the determination of the overall flux across the membrane, and give to this gas a behavior which differs from that of the other gases investigated. The further increase of the measured

permeability, in this concern, ca be explained by considering that the reduction of the tortuosity of the diffusion pathway caused by the disappearance of nylon crystals, affects more the permeability of diffusion controlled species, such as the small helium, than the one of other gases, whose flux seems to be controlled by solubility effects.

In general, the overall results confirmed that the benzoyl group, even if in small amount, positively affects the permselective properties of the dense polymeric materials, even if in this case the improvements, in terms of CO_2 selectivity were not as remarkable as the one obtained by Meshkat et al. [47] that were able to increase both permeabilities and selectivity of this gas with respect to N_2. This fact is most likely related to the higher mobility of the carboxylic acid added in that work, that was not bound to the polymer chain, and to the presence of the acidic group that, by increasing system polarity, could further enhance the solubility of CO_2 with respect to that of other gases.

In addition to that, it is interesting to notice that reduction of the overall polymer crystallinity, which was expected to increase the polymer permeability, had a limited effect, as the reduction of Nylon crystallinity was somewhat counterbalanced by the increase of the PTMO one, which likely limited the overall permeability increment.

5 Conclusions

The modification of Pebax®2533 through the substitution of Nylon amide's hydrogen with a bulky benzoyl group was performed and the obtained product, named "Benzoyl-P2533" (BP2533), was characterized to investigated the changes in thermal properties, structure and gas permeability.

The success of the reaction was proved by FTIR and NMR analysis which also allowed to calculate the yield obtained for the different reaction protocols tested. In particular, it was seen that reaction could be controlled by tuning the reactant ratio and the reaction temperature, with substantially complete substitution reached at 60°C and a large excess of Benzoyl Chloride (10:1).

TGA showed that the modified material's thermal resistance was substantially unaffected for temperatures below 250°C. However, at higher temperature the BP2533 showed the degradation of the substituted group from 275 °C, while the degradation of the pristine Pebax started at 360°C. At the same time, however, the degradation of the main polymer chain of fully substituted BP2533 resulted to start at a temperature 20°C higher than that of the pristine material.

The DSC allowed to investigate the substitution effect on the crystallinity of the copolymer; results showed that the presence of benzoyl group, prevented the crystallization of Polyamide12 phase, but at the same time increased the amount of polyether (PTMO) crystals, from 19% of the neat Pebax®2533 to a maximum of 35% for fully substituted BP2533.

The substitution also affected the material gas transport properties: compared to the pristine Pebax®2533, the overall permeability of the system increased for all gases of about 11-12 % without affecting their selectivity versus CO_2. Helium was the only exception: in this case indeed permeability increased of 48% along with a decrement of CO_2/He selectivity of 25%.

In conclusion, the modification carried on in this work led to a slight improvement of the overall permselective properties, since permeabilities of al gases increased, without compromise the CO_2

selectivity at all, with the only exception of helium. This difference seems to be related to the lower kinetic diameter of helium whose diffusivity seems more affected by crystallinity changes caused by Pebax modification.

Despite the limited improvements of the materials perm-selective properties, the approach adopted revealed a new possibility for matrix modification, that can be carried out using different groups as well, obtaining further improvements of the material. This work therefore could be a starting point for the investigation of many more Pebax (and not only) matrix modifications which can increase their intrinsic properties of the materials or tune their compatibility with high performance fillers in order to optimize them for gas separation as well as for other kind of applications.

Acknowledgements

This work has been performed in the framework of the European Project H2020 NANOMEMC 2 "NanoMaterials Enhanced Membranes for Carbon Capture", funded by the Innovation and Networks Executive Agency (INEA) Grant Agreement Number: 727734.

Declaration of interests

The authors declare that they have no known competing financial interests or personal relationships that could have appeared to influence the work reported in this paper.

Bibliography

[1] https://www.extrememateriials-arkema.com/en/product-families/pebax-elastomer-family/ last accessed 27/05/2021

[2] N. Deluca, PEBA: TPE materials for high performance applications, in: Annu. Tech. Conf. - ANTEC, Conf. Proc., Anaheim, CA, USA, 8–10 May 2017, n.d.: pp. 2343–2393.

[3] J.R. Flesher, Pebax® Polyether Block Amide — A New Family of Engineering Thermoplastic Elastomers, in: High Performance Polymers: Their Origin and Development. Proceedings of the Symposium on the History of High Performance Polymers at the American Chemical Society Meeting, New York, April 15–18, 1986, pp 401-408

[4] J. P. Sheth, J. Xu, G. L. Wilkes, Solid state structure–property behavior of semicrystalline poly(ether-block-amide) PEBAX® thermoplastic elastomers, Polymer, 44 (2003) 743-756

[5] J. Ahmad, W. U. Rehman, K. Deshmukh, S. K. Basha, B. Ahamed, K. Chidambaram, Recent Advances in Poly (Amide-B-Ethylene) Based Membranes for Carbon Dioxide (CO_2) Capture: A Review, Polymer-Plastics Technology and Materials, 58 (2019) , 366-383, DOI: 10.1080/03602559.2018.1482921

[6] S. Sridhar, S. Bee, S. Bhargava, Membrane-based Gas Separation: Principle, Applications and Future Potential, Chem. Eng. Dig. 1 (2014) 1–25.

[7] W.S.. Han, Y.; Ho, Recent advances in polymeric membranes for CO2 capture, Chinese J. Chem. Eng. 26 (2018) 2238–2254. doi:10.1016/j.cjche.2018.07.010.
[8] I. Sreedhar, R. Vaidhiswaran, B.M. Kamani, A. Venugopal, Process and engineering trends in membrane based carbon capture, Renew. Sustain. Energy Rev. 68 (2017) 659–684. doi:10.1016/j.rser.2016.10.025.
[9] R. Khalilpour, K. Mumford, H. Zhai, A. Abbas, G. Stevens, E.S. Rubin, Membrane-based carbon capture from flue gas: A review, J. Clean. Prod. 103 (2015) 286–300. doi:10.1016/j.jclepro.2014.10.050.
[10] P.R.S. Masson-Delmotte, V., P. Zhai, H.-O. Pörtner, D. Roberts, J. Skea, T.M. A. Pirani, W. Moufouma-Okia, C. Péan, R. Pidcock, S. Connors, J.B.R. Matthews, Y. Chen, X. Zhou, M.I. Gomis, E. Lonnoy, and T.W. M. Tignor, Global warming of 1.5°C, 2019. doi:10.1038/291285a0.
[11] UNFCCC, Paris Agreement, Conf. Parties Its Twenty-First Sess. 21932 (2015) 32. doi:FCCC/CP/2015/L.9/Rev.1.
[12] K. Dalane, Z. Dai, G. Mogseth, M. Hillestad, L. Deng, Potential applications of membrane separation for subsea natural gas processing: A review, J. Nat. Gas Sci. Eng. 39 (2017) 101–117. doi:10.1016/j.jngse.2017.01.023.
[13] C.A. Scholes, G.W. Stevens, S.E. Kentish, Membrane gas separation applications in natural gas processing, Fuel. 96 (2012) 15–28. doi:10.1016/j.fuel.2011.12.074.
[14] Y. Zhang, J. Sunarso, S. Liu, R. Wang, Current status and development of membranes for CO2/CH4 separation: A review, Int. J. Greenh. Gas Control. 12 (2013) 84–107. doi:10.1016/j.ijggc.2012.10.009.
[15] L.M. Robeson, The upper bound revisited, J. Memb. Sci. 320 (2008) 390–400. doi:10.1016/j.memsci.2008.04.030.
[16] P.S. Goh, A.F. Ismail, S.M. Sanip, B.C. Ng, M. Aziz, Recent advances of inorganic fillers in mixed matrix membrane for gas separation, 81 (2011) 243–264. doi:10.1016/j.seppur.2011.07.042.
[17] B. Sasikumar, G. Arthanareeswaran, A.F. Ismail, Recent progress in ionic liquid membranes for gas separation, J. Mol. Liq. 266 (2018) 330–341. doi:10.1016/j.molliq.2018.06.081.
[18] M. Vinoba, M. Bhagiyalakshmi, Y. Alqaheem, A.A. Alomair, A. Pérez, M.S. Rana, Recent progress of fillers in mixed matrix membranes for CO2 separation: A review, Sep. Purif. Technol. 188 (2017) 431–450. doi:10.1016/j.seppur.2017.07.051.
[19] A. Soleimany, S.S. Hosseini, F. Gallucci, Recent progress in developments of membrane materials and modification techniques for high performance helium separation and recovery: A review, Chem. Eng. Process. Process Intensif. 122 (2017) 296–318. doi:10.1016/j.cep.2017.06.001.
[20] M. Wang, Z. Wang, S. Zhao, J. Wang, S. Wang, Recent advances on mixed matrix membranes for CO2 separation, Chinese J. Chem. Eng. 25 (2017) 1581–1597. doi:10.1016/j.cjche.2017.07.006.
[21] M.A. Aroon, A.F. Ismail, T. Matsuura, M.M. Montazer-Rahmati, Performance studies of mixed matrix membranes for gas separation: A review, Sep. Purif. Technol. 75 (2010) 229–242. doi:10.1016/j.seppur.2010.08.023.
[22] P.S. Goh, A.F. Ismail, S.M. Sanip, B.C. Ng, M. Aziz, Recent advances of inorganic fillers in mixed matrix membrane for gas separation, Sep. Purif. Technol. 81 (2011) 243–264. doi:10.1016/j.seppur.2011.07.042.
[23] R. Casadei, D. Venturi, M.G. Baschetti, L. Giorgini, E. Maccaferri, S. Ligi, Polyvinylamine membranes containing graphene-based nanofillers for carbon capture applications, Membranes (Basel). 9 (2019) 20. doi:10.3390/membranes9090119.
[24] X. Yan, S. Anguille, M. Bendahan, P. Moulin, Ionic liquids combined with membrane separation processes: A review, Sep. Purif. Technol. 222 (2019) 230–253. doi:10.1016/j.seppur.2019.03.103.

[25] L. Ansaloni, J.R. Nykaza, Y. Ye, Y.A. Elabd, M. Giacinti Baschetti, Influence of water vapor on the gas permeability of polymerized ionic liquids membranes, J. Memb. Sci. 487 (2015) 199–208. doi:10.1016/j.memsci.2015.03.065.
[26] L.A. Neves, J.G. Crespo, I.M. Coelhoso, Gas permeation studies in supported ionic liquid membranes, J. Memb. Sci. 357 (2010) 160–170. doi:10.1016/j.memsci.2010.04.016.
[27] B. Sasikumar, G. Arthanareeswaran, A.F. Ismail, Recent progress in ionic liquid membranes for gas separation, J. Mol. Liq. 266 (2018) 330–341. doi:10.1016/j.molliq.2018.06.081.
[28] L. Ansaloni, Y. Zhao, B.T. Jung, K. Ramasubramanian, M.G. Baschetti, W.S.W. Ho, Facilitated transport membranes containing amino-functionalized multi-walled carbon nanotubes for high-pressure CO2 separations, J. Memb. Sci. 490 (2015) 18–28. doi:10.1016/j.memsci.2015.03.097.
[29] Y. Chen, W.S.W. Ho, High-molecular-weight polyvinylamine/piperazine glycinate membranes for CO2 capture from flue gas, J. Memb. Sci. 514 (2016) 376–384. doi:10.1016/j.memsci.2016.05.005.
[30] V. Vakharia, W. Salim, D. Wu, Y. Han, Y. Chen, L. Zhao, W.S.W. Ho, Scale-up of amine-containing thin-film composite membranes for CO2 capture from flue gas, J. Memb. Sci. 555 (2018) 379–387. doi:10.1016/j.memsci.2018.03.074.
[31] D. Venturi, D. Grupkovic, L. Sisti, M.G. Baschetti, Effect of humidity and nanocellulose content on Polyvinylamine-nanocellulose hybrid membranes for CO2capture, J. Memb. Sci. 548 (2018) 263–274. doi:10.1016/j.memsci.2017.11.021.
[32] D. Venturi, A. Chrysanthou, B. Dhuiège, K. Missoum, M.G. Baschetti, Arginine/Nanocellulose membranes for carbon capture applications, Nanomaterials. 9 (2019) 877. doi:10.3390/nano9060877.
[33] W. Yave, A. Car, K.-V. Peinemann, Nanostructured membrane material designed for carbon dioxide separation, J. Memb. Sci. 350 (2010) 124–129
[34] H. Lin, T. Kai, B. D. Freeman, S. Kalakkunnath, D.S. Kalika, The Effect of Cross-Linking on Gas Permeability in Cross-Linked Poly(Ethylene Glycol Diacrylate) Macromolecules 38 (2005) 20, 8381–8393 https://doi.org/10.1021/ma0510136
[35] J. Deng, Z. Dai, J. Yan, M. Sandru, E. Sandru, R. J. Spontak, L. Deng, Facile and solvent-free fabrication of PEG-based membranes with interpenetrating networks for CO2 separation, J. of Memb. Sci. 570–571(2019) 455-463, https://doi.org/10.1016/j.memsci.2018.10.031.
[36] N. P. Patel, M. A. Hunt, S. Lin-Gibson, S. Bencherif, R. J. Spontak, Tunable CO2 transport through mixed polyether membranes, J. Membr. Sci., 251 (2005) 51-57, https://doi.org/10.1016/j.memsci.2004.11.003.
[37] D.M. Muñoz, E.M. Maya, J. de Abajo, J. G. de la Campa, A. E. Lozano, Thermal treatment of poly(ethylene oxide)-segmented copolyimide based membranes: An effective way to improve the gas separation properties. J. Membr. Sci. 323 (2008) 53–59.
[38] A. Tena, A. Marcos-Fernández, A.E. Lozano, J. de Abajo, L. Palacio, L. P. Prádanos, A. Hernández, Influence of the PEO length in gas separation properties of segregating aromatic–aliphatic copoly(ether-imide)s. Chem. Eng. Sci. 104 (2013) 574–585.
[39] M. Minelli, M. Giacinti Baschetti, D. T. Hallinan, N. P. Balsara (2013). Study of gas permeabilities through polystyrene-block-poly(ethylene oxide) copolymers. J. Membr. Sci. 432 (2013) 83-89, doi:10.1016/j.memsci.2012.12.038
[40] A. Jomekian, B. Bazooyar, R.M. Behbahani, T. Mohammadi, A. Kargari, Ionic liquid-modified Pebax® 1657 membrane filled by ZIF-8 particles for separation of CO2 from CH4, N2 and H2, J. Memb. Sci. 524 (2017) 652–662. doi:10.1016/j.memsci.2016.11.065.
[41] M.M. Rahman, V. Filiz, S. Shishatskiy, C. Abetz, S. Neumann, S. Bolmer, M.M. Khan, V. Abetz, PEBAX® with PEG functionalized POSS as nanocomposite membranes for CO2 separation, J. Memb. Sci. 437 (2013) 286–297. doi:10.1016/j.memsci.2013.03.001.
[42] W. Zheng, R. Ding, K. Yang, Y. Dai, X. Yan, G. He, ZIF-8 nanoparticles with tunable size

for enhanced CO2 capture of Pebax based MMMs, Sep. Purif. Technol. 214 (2019) 111–119. doi:10.1016/j.seppur.2018.04.010.
[43] J. Eun, S. Ki, Y. Hoon, H. Bum, Effect of PEG-MEA and graphene oxide additives on the performance of Pebax®1657 mixed matrix membranes for CO2 separation, J. Memb. Sci. 572 (2019) 300–308. doi:10.1016/j.memsci.2018.11.025.
[44] Y.C. Liu, C.Y. Chen, G.S. Lin, C.H. Chen, K.C.W. Wu, C.H. Lin, K.L. Tung, Characterization and molecular simulation of Pebax-1657-based mixed matrix membranes incorporating MoS2 nanosheets for carbon dioxide capture enhancement, J. Memb. Sci. 582 (2019) 358–366. doi:10.1016/j.memsci.2019.04.025.
[45] H. Sanaeepur, R. Ahmadi, A. Ebadi Amooghin, D. Ghanbari, A novel ternary mixed matrix membrane containing glycerol-modified poly(ether-block-amide) (Pebax 1657)/copper nanoparticles for CO2 separation, J. Memb. Sci. 573 (2019) 234–246. doi:10.1016/j.memsci.2018.12.012.
[46] J. Wang, W. Fang, J. Luo, M. Gao, Y. Wan, S. Zhang, X. Zhang, A.H.A. Park, Selective separation of CO2 using novel mixed matrix membranes based on Pebax and liquid-like nanoparticle organic hybrid materials, J. Memb. Sci. 584 (2019) 79–88. doi:10.1016/j.memsci.2019.04.079.
[47] S. Meshkat, S. Kaliaguine, D. Rodrigue, Enhancing CO2 separation performance of Pebax® MH-1657 with aromatic carboxylic acids, Sep. Purif. Technol. 212 (2019) 901–912. doi:10.1016/j.seppur.2018.12.008.
[48] L. Dong, M. Chen, J. Li, D. Shi, W. Dong, X. Li, Y. Bai, Metal-organic framework-graphene oxide composites : A facile method to highly improve the CO2 separation performance of mixed matrix membranes, J. Memb. Sci. 520 (2016) 801–811. doi:10.1016/j.memsci.2016.08.043.
[49] J.M.P. Scofield, P.A. Gurr, J. Kim, Q. Fu, S.E. Kentish, G.G. Qiao, Development of novel fluorinated additives for high performance CO2 separation thin-film composite membranes, J. Memb. Sci. 499 (2016) 191–200. doi:10.1016/j.memsci.2015.10.035.
[50] V. Nafisi, M.B. Hägg, Development of nanocomposite membranes containing modified Si nanoparticles in PEBAX-2533 as a block copolymer and 6FDADurene diamine as a glassy polymer, ACS Appl. Mater. Interfaces. 6 (2014) 15643–15652. doi:10.1021/am500532a.
[51] V. Nafisi, M.B. Hägg, Development of dual layer of ZIF-8/PEBAX-2533 mixed matrix membrane for CO2 capture, J. Memb. Sci. 459 (2014) 244–255. doi:10.1016/j.memsci.2014.02.002.
[52] R. Casadei, M.G. Baschetti, M.J. Yoo, H.B. Park, L. Giorgini, Pebax® 2533/graphene oxide nanocomposite membranes for carbon capture, Membranes. 10 (2020) 1–20. doi:10.3390/membranes10080188.
[53] H. Yuan, X. Liu, S. Zhang, J. Lu, Pervaporative desulfurization of n-heptane/thiophene model gasoline for modified polyether-block-amide (Pebax) membrane, Chem. Eng. Process. - Process Intensif. 144 (2019) 107632. doi:10.1016/j.cep.2019.107632
[54] E. V. Konyukhova, A.I. Buzin, Y.U.K. Godovsky, Melting of polyether block amide (pebax): The effect of stretching, Thermochim. Acta. 391 (2002) 271–277. doi:10.1016/S0040-6031(02)00189-2.
[55] J.C.I. Lara-estévez, L. Antônio, S. De Almeida, K. Schulte, E. Bucio, PEBAX TM-Silanized Al2O3 Composite, Synthesis and Characterization, Open J. Polym. Chem. 2 (2012) 63–69.
[56] S. Armstrong, B. Freeman, A. Hiltner, E. Baer, Gas permeability of melt-processed poly (ether block amide) copolymers and the effects of orientation, Polymer. 53 (2012) 1383–1392. doi:10.1016/j.polymer.2012.01.037.
[57] K. Liu, C. Fang, Z. Li, M. Young, Separation of thiophene / n-heptane mixtures using PEBAX / PVDF-composited membranes via pervaporation, J. Memb. Sci. 451 (2014) 24–31. doi:10.1016/j.memsci.2013.09.045.
[58] S.C.C. Gabriele Clarizia, Paola Bernardo, Giuliana Gorrasi, Daniela Zampino, Influence of

the Preparation Method and Photo-Oxidation Treatment on the Thermal and Gas Transport Properties of Dense Films Based on a, (2018). doi:10.3390/ma11081326.
[59] M.S.A. Wahab, A.R. Sunarti, Development of PEBAX Based Membrane for Gas Separation : A Review, Int. J. Membr. Sci. Tech., 2 (2015) 78–84.
[60] L. J. Fang, J. H. Chen, J. M. Wang, W. W. Lin, X. G. Lin, Q. J. Lin, and Y. S. He, Hydrophobic Two-Dimensional MoS2 Nanosheets Embedded in a Polyether Copolymer Block Amide (PEBA) Membrane for Recovering Pyridine from a Dilute Solution, ACS Omega, 6 (2021), 2675–2685 https://doi.org/10.1021/acsomega.0c04852
[61] M.L. Bender, Mechanisms of Catalysis of Nucleophilic Reactions of Carboxylic Acid Derivatives. Chem. Rev. 60, (1960) 53–113 https://doi.org/10.1021/cr60203a005
[62] Robert J. Ouellette, J. David Rawn, 15 - Alcohols: Reactions and Synthesis,in Organic Chemistry, Robert J. Ouellette, J. David Rawn Editors, Elsevier, 2014, Pages 491-534,
[63] J. Catalano, T. Myezwa, M.G. De Angelis, M.G. Baschetti, G.C. Sarti, The effect of relative humidity on the gas permeability and swelling in PFSI membranes, Int. J. Hydrogen Energy. 37 (2012) 6308–6316. doi:10.1016/j.ijhydene.2011.07.047
[64] SigmaAldrich, IR Spectrum Table & Chart, (n.d.). https://www.sigmaaldrich.com/technical-documents/articles/biology/ir-spectrum-table.html.
[65] NIST - National Institute of Standards and Technology., NIST Benzoyl chloride - Infrared Spectrum, (n.d.). https://webbook.nist.gov/cgi/cbook.cgi?ID=C98884&Type=IR-SPEC&Index=2#IR-SPEC (accessed May 9, 2020).
[66] Pebax 2533 datasheet in https://www.campusplastics.com/campus/eng/datasheet/Pebax%C2%AE+2533+SD+02/ARKEMA/179/96f4997e last accessed 27/05/2021
[67] P. Chen, M. Tang, W. Zhu, L. Yang, S. Wen, C. Yan, Z. Ji, H. Nan, Y. Shi, Systematical mechanism of Polyamide-12 aging and its micro-structural evolution during laser sintering, Polym. Test. 67 (2018) 370–379. doi:10.1016/j.polymertesting.2018.03.035.
[68] L.J.L. Duddleston, A.T. Puck, A. Harris, N.P. Doll, T.A. Osswald, Differential scanning calorimetry (DSC) quantification of polyamide 12 (nylon 12) degradation during the selective laser sintering (SLS) process, Annu. Tech. Conf. - ANTEC, Conf. Proc. 12 (2016) 1–4.
[69] G.M. Craft, Characterization of Nylon-12 in a Novel Additive Manufacturing Technology , and the Rheological and Spectroscopic Analysis of PEG-Starch Matrix Interactions by, 2018.
[70] A. Dorigato, M. Brugnara, A. Pegoretti, Novel polyamide 12 based nanocomposites for industrial applications, J. Polym. Res. 24 (2017) 1–13. doi:10.1007/s10965-017-1257-9.
[71] J. Zhang, A. Adams, Understanding thermal aging of non-stabilized and stabilized polyamide 12 using 1H solid-state NMR, Polym. Degrad. Stab. 134 (2016) 169–178. doi:10.1016/j.polymdegradstab.2016.10.006.
[72] S. Gogolewski, K. Czerniawska, M. Gasiorek, Effect of annealing on thermal properties and crystalline structure of polyamides. Nylon 12 (polylaurolactam), 1136 (1980) 1130–1136
[73] B. Grassl, B. Meurer, M. Scheer, J.C. Galin, Segmented Poly(tetramethylene oxide) Zwitterionomers and Their Homologous Ionenes. 2. Phase Separation through DSC and Solid State 1H-NMR Spectroscopy, Macromolecules. 30 (1997) 236–245.